



Turing–Hopf bifurcation and spatiotemporal patterns in a Gierer–Meinhardt system with gene expression delay*

Shuangrui Zhao , Hongbin Wang , Weihua Jiang 

School of Mathematics, Harbin Institute of Technology,
Harbin 150001, China

wanghb@hit.edu.cn; jiangwh@hit.edu.cn

Received: February 10, 2020 / **Revised:** September 22, 2020 / **Published online:** May 1, 2021

Abstract. In this paper, we consider the dynamics of delayed Gierer–Meinhardt system, which is used as a classic example to explain the mechanism of pattern formation. The conditions for the occurrence of Turing, Hopf and Turing–Hopf bifurcation are established by analyzing the characteristic equation. For Turing–Hopf bifurcation, we derive the truncated third-order normal form based on the work of Jiang et al. [11], which is topologically equivalent to the original equation, and theoretically reveal system exhibits abundant spatial, temporal and spatiotemporal patterns, such as semistable spatially inhomogeneous periodic solutions, as well as tristable patterns of a pair of spatially inhomogeneous steady states and a spatially homogeneous periodic solution coexisting. Especially, we theoretically explain the phenomenon that time delay inhibits the formation of heterogeneous steady patterns, found by S. Lee, E. Gaffney and N. Monk [The influence of gene expression time delays on Gierer–Meinhardt pattern formation systems, *Bull. Math. Biol.*, 72(8):2139–2160, 2010.]

Keywords: Gierer–Meinhardt system, delay, Turing–Hopf bifurcation, normal form, spatiotemporal patterns.

1 Introduction

In developmental biology, embryonic development is mediated by morphogens. It is a signal molecule that determines the location, differentiation and fate of many surrounding cells [9]. In [26], Turing showed that two diffusible morphogens could instigate diffusion-driven symmetry breaking and bifurcation. Diffusion can destroy the stability of spatial homogeneous steady state, that is, the stability process can evolve into an instability with diffusion effect. Since then, a large amount of literature research on Turing instability mechanism has emerged in developmental biology. A fundamental property for instabilities in such systems is short-range activation and long-range inhibition [13]. In developmental biology, the Gierer–Meinhardt model is used as a classic example to explain

*This research was supported by the National Natural Science Foundation of China (No. 11871176).

the mechanism of pattern formation. The so-called Gierer–Meinhardt model is [6]

$$\begin{aligned} \frac{\partial u(x, t)}{\partial t} &= D_u \frac{\partial^2 u(x, t)}{\partial x^2} + \rho \rho_0 + c \rho \frac{u^2(x, t)}{v(x, t)} - \mu u(x, t), \quad x \in (0, l\pi), t > 0, \\ \frac{\partial v(x, t)}{\partial t} &= D_v \frac{\partial^2 v(x, t)}{\partial x^2} + c' \rho' u^2(x, t) - \nu v(x, t), \quad x \in (0, l\pi), t > 0, \\ u_x(0, t) &= u_x(l\pi, t) = v_x(0, t) = v_x(l\pi, t) = 0, \quad t > 0, \\ u(x, 0) &= \phi_1(x, 0) \geq 0, \quad v(x, 0) = \phi_2(x, 0) \geq 0, \quad x \in [0, l\pi], \end{aligned} \quad (1)$$

where $u(x, t)$ and $v(x, t)$ are concentrations of activator and inhibitor at (x, t) , respectively, and $l, D_u, D_v, \rho, \rho', \rho_0, \mu, \nu, c, c'$ are all positive constants.

Numerous studies have been done for model (1). The detailed stability and diffusion-driven instability, i.e., Turing instability of such system are provided in [21, 28]. These results further theoretically verify Turing's idea. The sufficient conditions for the occurrence of Hopf bifurcation is performed in [18] showing the existence of spatially homogeneous periodic solutions. Recently, Yang et al. [29] have investigated the conditions for the existence of Turing–Hopf bifurcation to reveal the system exhibits various spatiotemporal patterns.

Sakuma et al. [22] have emphasized the role of gene expression in morphogenesis utilizing in situ hybridization, which records mRNA levels as illustrated in developmental self-organisation via Nodal and Lefty gene products in zebrafish mesodermal induction. The timescales of transcriptional and translational are estimated to be in the range of 10 minutes to several hours [16]. However, previous studies usually ignore the role of gene expression delays caused by transcription and translation in kinetics. Therefore, a diffusive Gierer–Meinhardt system with time delay is proposed in [15] as follows:

$$\begin{aligned} \frac{\partial u(x, t)}{\partial t} &= D_u \frac{\partial^2 u(x, t)}{\partial x^2} + \rho \rho_0 + c \rho \frac{u^2(x, t - \tau)}{v(x, t - \tau)} - \mu u(x, t), \quad x \in (0, l\pi), t > 0, \\ \frac{\partial v(x, t)}{\partial t} &= D_v \frac{\partial^2 v(x, t)}{\partial x^2} + c' \rho' u^2(x, t - \tau) - \nu v(x, t), \quad x \in (0, l\pi), t > 0, \\ u_x(0, t) &= u_x(l\pi, t) = v_x(0, t) = v_x(l\pi, t) = 0, \quad t > 0, \\ u(x, t) &= \phi_1(x, t) \geq 0, \quad v(x, t) = \phi_2(x, t) \geq 0, \quad (x, t) \in [0, l\pi] \times [-\tau, 0]. \end{aligned} \quad (2)$$

The two activators molecules can reversibly bind to a receptor and eventually induce the production of additional activator (or inhibitor) molecules, but this production has been delayed for period of time τ . For simplicity, we assume throughout time delay of both gene expression events is same and constant [15].

A large number of literature studies show that dynamics depends crucially on the time delay parameter. Time delay will destroy the stability of the steady state and lead to a temporally periodic solution, that is, the Hopf bifurcation occurs [3, 8, 19, 20]. In [2], Chen et al. have studied the Hopf bifurcation analysis for model (2). It is proved that system possesses temporal pattern. Lee et al. [15] have explored the influence of gene expression time delays on pattern formation, what is more, proved that the delayed Gierer–Meinhardt model exhibits abundant Turing pattern through numerical simulation.

Furthermore, in this paper, we will focus on the joint effect of diffusion and time delay on the pattern for model (2). It is noted that Jiang et al. [12] have mainly considered the impact of diffusion and delay on the Schnakenberg model, which arises from simple chemical reaction systems with limit cycle behavior [23], and found that the system exhibits affluent dynamic behavior (the unfoldings for normal forms at Turing–Hopf singularity are case Ia and case III according to [7]). We observe that the Gierer–Meinhardt model has more complex nonlinear terms and based on the work of Lee et al. [15] in which revealed model exhibits numerous interesting Turing pattern by numerical simulation. Therefore, these findings have inspired us to study the Gierer–Meinhardt model to explore how diffusion and delay essentially affect the formation of pattern and whether the model can produce more complex Turing patterns comparing with the Schnakenberg model.

In this paper, we will build the existence of Turing, Hopf and Turing–Hopf bifurcation for the delayed Gierer–Meinhardt model. Firstly, we get the Turing bifurcation curve by analyzing the characteristic equation, which is continuous and piecewise smooth, and system undergoes Turing–Turing bifurcation at the nonsmooth points. Especially, we obtain the spatial inhomogeneous steady state in multifarious profiles, which depends on the wave number. This provides a theoretical explanation for the existence of spatial inhomogeneous periodic solutions with high frequency at low diffusion rates. Next, we take time delay as the bifurcation parameter proving that the model will undergo Hopf bifurcation at critical values. It is worth mentioning that characteristic equation contains a second-order transcendental term, which results in solving the parameter values for the purely imaginary eigenvalues $\pm iw$ is reduced to an eighth-order polynomial of w , hence the critical parameter values can hardly be explicitly solved. Finally, we will mainly focus on the interaction of diffusion and delay on the model from the perspective of Turing–Hopf by method of combining the central manifold theorem and the normal form theory [4, 5, 10, 27]. It is worth noting that codimension-2 Turing–Hopf bifurcation is usually to be applied to explain spatiotemporal phenomena in chemical reaction, predator–prey models, developmental biology, etc. [1, 12, 24, 25, 29, 30]. Jiang et al. [11] have derived the formulas of calculating normal forms for a general delayed reaction diffusion equation with Neumann boundary condition, which can greatly simplify the complexity of calculation. By employing these formulas we theoretically prove the existence of various spatiotemporal patterns instead of computational simulations [14, 15], such as semistable spatially inhomogeneous periodic solutions, as well as tristability of a pair of spatially inhomogeneous steady states and a spatially homogeneous periodic solution coexisting, in addition, quantitatively give the specific existence region of various forms of solutions near the Turing–Hopf singularity.

This paper is organized as follows. In Section 2, by analyzing characteristic equations at the positive constant steady state we have established the conditions for Turing, Hopf and Turing–Hopf bifurcation. In Section 3, normal forms truncated to order 3 of the delayed Gierer–Meinhardt systems in the neighborhood of Turing–Hopf singularity are derived by applying normal form method [4, 27] and generic formulas evolved in [11]. In Section 4, we analyze the reduced Gierer–Meinhardt systems with gene expression delay and present that the systems exhibits various interesting spatial, temporal and spatiotemporal patterns. Moreover, numerical simulations are shown to illustrate the previous

theoretical results. Finally, there is a brief conclusion in Section 5. Throughout the paper, \mathbb{N} is the set of all positive integers, and $\mathbb{N}_0 = \mathbb{N} \cup \{0\}$ represents the set of all nonnegative integers.

2 Turing Bifurcation and Hopf bifurcation

In this section, we consider the Turing bifurcation and Hopf bifurcation for system (2) with the homogeneous Neumann boundary condition.

For the sake of convenience, by applying the following scalings [15]:

$$\begin{aligned} \tilde{t} &= \frac{t}{T_s}, & \tilde{\tau} &= \frac{\tau}{T_s}, & \tilde{x} &= \frac{x}{l}, & \tilde{\gamma} &= T_s \nu, \\ \tilde{D} &= \frac{T_s D_v}{l^2}, & \tilde{u} &= \frac{c' \rho'}{c \rho} u, & \tilde{v} &= \frac{c' \rho' \nu}{c^2 \rho^2} v, \end{aligned}$$

where T_s is a arbitrary timescale. Dropping the tilde, system (2) becomes the following nondimensionalized system:

$$\begin{aligned} \frac{\partial u(x, t)}{\partial t} &= \varepsilon D \frac{\partial^2 u(x, t)}{\partial x^2} + \gamma \left(p - qu(x, t) + \frac{u^2(x, t - \tau)}{v(x, t - \tau)} \right), & x \in (0, \pi), t > 0, \\ \frac{\partial v(x, t)}{\partial t} &= D \frac{\partial^2 v(x, t)}{\partial x^2} + \gamma (u^2(x, t - \tau) - v(x, t)), & x \in (0, \pi), t > 0, \\ u_x(0, t) &= u_x(\pi, t) = v_x(0, t) = v_x(\pi, t) = 0, & t > 0, \\ u(x, t) &= \phi_1(x, t) \geq 0, \quad v(x, t) = \phi_2(x, t) \geq 0, & (x, t) \in [0, \pi] \times [-\tau, 0], \end{aligned} \tag{3}$$

where $p = \rho_0 \rho' c' / (c \nu) > 0$, $q = \mu / \nu > 0$, $\varepsilon = D_u / D_v > 0$.

Obviously, there is a unique positive equilibrium $(u_*, v_*) = ((p+1)/q, ((p+1)/q)^2)$. Linearizing system (3) at (u_*, v_*) , we obtain

$$\begin{aligned} \frac{\partial u(x, t)}{\partial t} &= \varepsilon D \frac{\partial^2 u(x, t)}{\partial x^2} - \gamma \left(pu(x, t) + \frac{2q}{p+1} u(x, t - \tau) \right. \\ &\quad \left. - \frac{q^2}{(p+1)^2} v(x, t - \tau) \right), & x \in (0, \pi), t > 0, \\ \frac{\partial v(x, t)}{\partial t} &= D \frac{\partial^2 v(x, t)}{\partial x^2} - \gamma \left(v(x, t) - \frac{2(p+1)u(x, t - \tau)}{q} \right), & \\ x &\in (0, \pi), t > 0, \\ u_x(0, t) &= u_x(\pi, t) = v_x(0, t) = v_x(\pi, t), & t > 0, \\ u(x, t) &= \phi_1(x, t) \geq 0, \quad v(x, t) = \phi_2(x, t) \geq 0, & (x, t) \in [0, \pi] \times [-\tau, 0]. \end{aligned} \tag{4}$$

Let $\mu_k, k \in \mathbb{N}_0$, be the eigenvalue of Laplace operator $-\Delta$ with Neumann boundary condition in one dimensional spatial domain $(0, \pi)$. Then $\mu_k = k^2$ and the characteristic equation of (4) is

$$D_k(\lambda, \tau, \varepsilon) := \lambda^2 + p_k \lambda + r_k + (s_k \lambda + q_k) e^{-\lambda \tau} + h_k e^{-2\lambda \tau} = 0, \quad k \in \mathbb{N}_0, \tag{5}$$

where

$$\begin{aligned} p_k &= (\varepsilon + 1)Dk^2 + \gamma(1 + q), & r_k &= (\varepsilon Dk^2 + \gamma q)(Dk^2 + \gamma), \\ s_k &= -\frac{2q\gamma}{p+1}, & q_k &= -(Dk^2 + \gamma)\frac{2q\gamma}{p+1}, & h_k &= \frac{2q\gamma^2}{p+1}. \end{aligned} \tag{6}$$

In particular, for $\tau = 0$, (5) turns into

$$D_k(\lambda, 0, \varepsilon) = \lambda^2 - TR_k\lambda + DET_k = 0, \quad k \in \mathbb{N}_0, \tag{7}$$

where

$$\begin{aligned} DET_k &= \varepsilon(Dk^2)^2 + \left(\varepsilon\gamma + \gamma q - \frac{2q\gamma}{p+1}\right)Dk^2 + \gamma^2q, & k \in \mathbb{N}_0, \\ TR_k &= -(\varepsilon + 1)Dk^2 - \gamma(q + 1) + \frac{2q\gamma}{p+1}, & k \in \mathbb{N}_0. \end{aligned}$$

Throughout this paper, we assume that

$$(N0) \quad 1 > 2q/(p + 1) - q > 0.$$

By (N0) we know that all eigenvalues of (7) with $k = 0$ have negative real parts.

2.1 Turing bifurcation

For any $k \in \mathbb{N}$, define

$$\varepsilon_*(k, D) = \frac{(\frac{2q\gamma}{p+1} - \gamma q)Dk^2 - \gamma^2q}{(Dk^2)^2 + \gamma Dk^2}, \quad D > D_k \triangleq \frac{\gamma^2q}{(\frac{2q\gamma}{p+1} - \gamma q)k^2}.$$

Obviously, $DET_k = 0$ whenever $\varepsilon = \varepsilon_*(k, D)$. The following lemma gives the properties of $\varepsilon_*(k, D)$.

Lemma 1. *Suppose that (N0) holds. Then we have*

- (i) *For any fixed $k \in \mathbb{N}$, $\varepsilon = \varepsilon_*(k, D)$ reaches its maximum ε_{\max} at extreme point $D = D_m(k)$,*

$$D_m(k) \triangleq \frac{(\frac{2q\gamma}{p+1} - \gamma q)\gamma + 2\gamma^2q + \sqrt{(\frac{2q\gamma}{p+1} - \gamma q)\gamma + 2\gamma^2q + 4(\frac{2q\gamma}{p+1} - \gamma q)\gamma^3q}}{2(\frac{2q\gamma}{p+1} - \gamma q)k^2} > D_k,$$

and $\varepsilon_(k, D)$ is monotonically decreasing (increasing) in D for $D > D_m(k)$ ($D_k < D < D_m(k)$).*

- (ii) *For any $k \in \mathbb{N}$, the equation*

$$\varepsilon_*(k, D) = \varepsilon_*(k + 1, D), \quad D > 0,$$

has a unique root $D_{k, k+1} \in (D_m(k + 1), D_m(k))$ for D , which is given by

$$D_{k, k+1} = \frac{1}{2\left(\frac{2q\gamma}{p+1} - \gamma q\right)} \left[\gamma^2 q \left(\frac{1}{k^2} + \frac{1}{(k+1)^2} \right) + \sqrt{\gamma^4 q^2 \left(\frac{1}{k^2} + \frac{1}{(k+1)^2} \right)^2 + \frac{4\left(\frac{2q\gamma}{p+1} - \gamma q\right)\gamma^3 q}{k^2(k+1)^2}} \right].$$

Moreover,

$$\varepsilon_*(k, D) > \varepsilon_*(k + 1, D) > \varepsilon_*(k + 2, D) > \dots, \quad D > D_{k, k+1}.$$

In order to understand the properties of $\varepsilon_*(k, D)$ more intuitively, we give the graph of $\varepsilon_*(k, D)$ for different k in Fig. 1.

In the following, we define

$$\varepsilon_*(D) := \varepsilon_*(k, D), \quad D \in [D_{k, k+1}, D_{k-1, k}), \quad k \in \mathbb{N},$$

where $D_{0,1} := +\infty$. From the following analysis we will note that $\varepsilon_*(D)$ is actually the Turing bifurcation curve and $T_{k, k+1}$, $k \in \mathbb{N}$, is the Turing–Turing bifurcation points, which are plotted in Fig. 1. The properties of $\varepsilon_*(D)$ are similar to the Turing bifurcation curve in delayed Schnakenberg systems, in [12], it gives a detailed explanation so we can omit here.

Lemma 2. Assume that (N0) holds and $D > \gamma$. Then

- (i) If $D \in (D_{k_1, k_1+1}, D_{k_1-1, k_1})$ for some $k_1 \in \mathbb{N}$ and $\varepsilon = \varepsilon_*(D)$, then 0 is a simple root of (5) with $k = k_1$, and all the other roots of (5) have strictly negative parts for $\tau = 0$. Furthermore, Let $\lambda = \lambda(k, \tau, \varepsilon)$ be the root of (5) with $k = k_1$ such that $\lambda(k_1, \tau, \varepsilon_*(D)) = 0$. Then $d\lambda(k_1, \tau, \varepsilon)/d\varepsilon|_{\varepsilon=\varepsilon_*(D)} < 0$.
- (ii) If $D = D_{k_1, k_1+1}$, $\varepsilon = \varepsilon_*(D_{k_1, k_1+1})$, then 0 is a simple root of (5) for both k_1 and $k_1 + 1$.

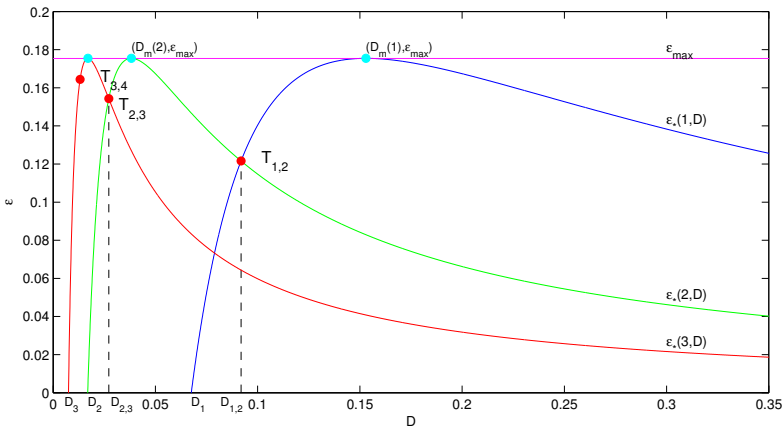


Figure 1. The curves of $\varepsilon_*(k, D)$ for different k , $k \in \mathbb{N}$.

Proof of Lemma 2. (i) $DET_k = 0$ if and only if $\varepsilon = \varepsilon_*(k, D)$ for $k \in \mathbb{N}$. So, for any $k \in \mathbb{N}$, $\lambda = 0$ is always a root of (5) with such k when $\varepsilon = \varepsilon_*(k, D)$. Then by the properties of $\varepsilon_*(D)$ and $\varepsilon_*(k, D)$, when $D \in (D_{k_1, k_1+1}, D_{k_1-1, k_1})$ for some k_1 and $\varepsilon = \varepsilon_*(D)$, $\lambda = 0$ is the root of (5) with $k = k_1$. Moreover, $\lambda = 0$ is simple, by $D > \gamma$ we can obtain that

$$\left. \frac{dD_{k_1}(\lambda, \tau, \varepsilon)}{d\lambda} \right|_{\lambda=0} = -TR_{k_1} + \tau(-q_{k_1} - 2h_{k_1}) > 0.$$

By (N0) we know that $TR_k < 0$ for all $k \in \mathbb{N}_0$ and $DET_k > 0$ for all $k \in \mathbb{N}$, $k \neq k_1$. So all the other roots of (5) for $\tau = 0$ has negative real parts when $\varepsilon = \varepsilon_*(D)$.

Differentiating (5) with respect to ε and due to $D > \gamma$, we can deduce that

$$\frac{d\lambda(k_1, \tau, \varepsilon_*(D))}{d\varepsilon} = -\frac{D^2k^4 + Dk^2\gamma}{p_{k_1} + s_{k_1} - \tau q_{k_1} - 2\tau h_{k_1}} < 0.$$

(ii) The proof is similar to proof of (i), which is omitted here. □

From the above analysis we can get the following important conclusions about Turing bifurcation of system (3).

Theorem 1. *Assume that (N0) holds and $D > \gamma$. Then*

- (i) *For $D > 0$, if $\varepsilon > \varepsilon_*(D)$, then (u_*, v_*) of system (3) is asymptotically stable for $\tau = 0$, and if $0 < \varepsilon < \varepsilon_*(D)$, then (u_*, v_*) is unstable.*
- (ii) *For $D \in (D_{k, k+1}, D_{k-1, k})$, system (3) will undergoes k -mode Turing bifurcation at $\varepsilon = \varepsilon_*(D)$.*
- (iii) *When $D = D_{k, k+1}$, $(k, k + 1)$ -mode Turing–Turing bifurcation occurs at $\varepsilon = \varepsilon_*(D_{k, k+1})$.*

Remark 1. The definition of k -mode Turing bifurcation, which occurs in the last theorem, as well as k_2 -mode Hopf bifurcation and (k_1, k_2) -mode Turing–Hopf bifurcation, which will occur in the following parts, are given on page 6 of [11]. A $(k, k + 1)$ -mode Turing–Turing bifurcation can be defined in the same manner as (k_1, k_2) -mode Turing–Hopf. The reader can refer to [12], so, it will not be repeated here.

2.2 Hopf bifurcation

In this section, we study the Hopf bifurcation in the case of $\varepsilon \geq \varepsilon_*(D)$, $D > 0$. We will employ the method proposed in [2] and [17] to analyze the distribution of characteristic roots of (5).

For some $k \in \mathbb{N}_0$, let $\lambda = i\omega_k$ ($\omega_k > 0$) satisfy $D_k(i\omega_k, \tau, \varepsilon) = 0$, then we have

$$-w_k^2 + p_k w_k i + r_k + (s_k w_k i + q_k) e^{-i\omega_k \tau} + h_k e^{-2i\omega_k \tau} = 0.$$

If $\omega_k \tau / 2 \neq \pi / 2 + j\pi$, $j \in \mathbb{Z}$, then let $\theta_k = \tan(\omega_k \tau / 2)$, and we have $e^{-i\omega_k \tau} = (1 - i\theta_k) / (1 + i\theta_k)$. Separating the real and imaginary parts, we have

$$\begin{aligned} (w_k^2 - r_k + q_k - h_k)\theta_k^2 - 2p_k w_k \theta_k &= w_k^2 - r_k - q_k - h_k, \\ (s_k - p_k)w_k \theta_k^2 + (-2w_k^2 + 2r_k - 2h_k)\theta_k &= -(p_k + s_k)w_k. \end{aligned} \tag{8}$$

Denote

$$M_1 = \begin{pmatrix} w_k^2 - r_k - q_k - h_k & -2p_k w_k \\ -(p_k + s_k)w_k & -2w_k^2 + 2r_k - 2h_k \end{pmatrix},$$

$$M_2 = \begin{pmatrix} w_k^2 - r_k + q_k - h_k & w_k^2 - r_k - q_k - h_k \\ (s_k - p_k)w_k & -(p_k + s_k)w_k \end{pmatrix}$$

and

$$M_3 = \begin{pmatrix} w_k^2 - r_k + q_k - h_k & -2p_k w_k \\ (s_k - p_k)w_k & -2w_k^2 + 2r_k - 2h_k \end{pmatrix}.$$

We define

$$E(w_k) = \det(M_1), \quad F(w_k) = \det(M_2) \quad \text{and} \quad D(w_k) = \det(M_3).$$

If $D(w_k) \neq 0$, then we can solve from (8) that

$$\theta_k^2 = \frac{E(w_k)}{D(w_k)}, \quad \theta_k = \frac{F(w_k)}{D(w_k)}, \quad (9)$$

and from (9) we find that w_k satisfied

$$D(w_k)E(w_k) = F(w_k)^2. \quad (10)$$

If $D(w_k) = 0$, in order to make sure the solvability of (8) for θ , then we have

$$E(w_k) = F(w_k) = 0,$$

and hence w_k satisfies (10) in this case as well. Simplifying (10), we conclude that w_k satisfies a polynomial equation with degree 8:

$$w_k^8 + e_3^k w_k^6 + e_2^k w_k^4 + e_1^k w_k^2 + e_0^k = 0, \quad (11)$$

where

$$e_3^k = -4r_k + 2p_k^2 - s_k^2,$$

$$e_2^k = 6r_k^2 - 2h_k^2 + p_k^4 - 4p_k^2 r_k - q_k^2 - s_k^2 p_k^2 + 2s_k^2 r_k + 2s_k^2 h_k,$$

$$e_1^k = -4r_k^3 + 4r_k h_k^2 + 2p_k^2 r_k^2 - 2p_k^2 h_k^2 + 2q_k^2 r_k - 2q_k^2 h_k$$

$$+ 4s_k q_k p_k h_k - s_k^2 r_k^2 - s_k^2 h_k^2 - 2s_k^2 r_k h_k - q_k^2 p_k^2,$$

$$e_0^k = r_k^4 - 2r_k^2 h_k^2 + h_k^4 - q_k^2 r_k^2 - q_k^2 h_k^2 + 2q_k^2 r_k h_k,$$

and $z_k = w_k^2$ is a positive root of

$$h(z_k) \triangleq z_k^4 + e_3^k z_k^3 + e_2^k z_k^2 + e_1^k z_k + e_0^k = 0. \quad (12)$$

If $w_k \tau / 2 = \pi / 2 + j\pi$, $j \in \mathbb{Z}$, then $p_k = s_k$, $w_k^2 = r_k + h_k - q_k$, and hence $D(w_k) = F(w_k) = 0$. So w_k^2 is still a positive root of (12). From the above analysis we have the following lemma.

Lemma 3. For $k \in \mathbb{N}_0$, if $\pm iw_k$ ($w_k > 0$) satisfies $D_k(\pm iw_k, \tau, \varepsilon) = 0$, then $h(w_k^2) = 0$.

If we can give the conditions under which the converse of Lemma 3 is true, then we have obtained the purely imaginary roots of the characteristic equation (5). In [2], Chen et al. provided an effective method to solve this problem. Denote

$$\mathcal{G}(w_k, \theta_k) = [q_k(1 + \theta_k^2) + 2h_k(1 - \theta_k^2)] \cdot [2w_k(1 - \theta_k^2) + 2p_k\theta_k] - [s_k w_k(1 + \theta_k^2) - 4h_k\theta_k] \cdot [p_k(1 - \theta_k^2) - 4w_k\theta_k + s_k(1 + \theta_k^2)].$$

Therefore, we obtain the following lemma.

Lemma 4. (See [2].) For $k \in \mathbb{N}_0$, there is $w_k > 0$ satisfying $h(w_k^2) = 0$, $D(\omega_k) \neq 0$ and $\mathcal{G}(w_k, \theta_k) \neq 0$, then $\pm i\omega_k$ are a simple pair of purely imaginary roots of (5) when

$$\tau = \tau_k^{(j)} = \frac{2 \arctan \theta_k + 2j\pi}{\omega_k}, \quad j \in \mathbb{Z},$$

where $\theta_k = F(\omega_k)/D(\omega_k)$ with $\omega = \omega_k$. Moreover, for $\theta_k \in (-\infty, \infty)$, there exists $\lambda(\tau) = \alpha(\tau) + iw(\tau)$, which is the unique root of (5) for $\tau \in (\tau_k^{(j)} - \epsilon, \tau_k^{(j)} + \epsilon)$ for some small $\epsilon > 0$ satisfying $\alpha(\tau_k^{(j)}) = 0$ and $w(\tau_k^{(j)}) = w_k$, in addition,

$$\left. \frac{d\alpha(\tau)}{d\tau} \right|_{\tau=\tau_k^{(j)}} > 0 \quad \text{when } \mathcal{G}(w_k, \theta_k) > 0,$$

$$\left. \frac{d\alpha(\tau)}{d\tau} \right|_{\tau=\tau_k^{(j)}} < 0 \quad \text{when } \mathcal{G}(w_k, \theta_k) < 0.$$

For $\theta_k = \infty$ (in the sense that $\arctan \theta_k = \pi/2 + j\pi, j \in \mathbb{Z}$), if $2h_k - q_k \neq 0$, we have the same result.

In order to discuss the existence of the positive root of the (12), we have adopted the method in [17].

For $h(z_k)$ of (12), we have $h'(z_k) = 4z_k^3 + 3e_3^k z_k^2 + 2e_2^k z_k + e_1^k$. Set

$$4z_k^3 + 3e_3^k z_k^2 + 2e_2^k z_k + e_1^k = 0. \tag{13}$$

Let $y = z_k + e_3^k/4$. Then (13) becomes

$$y^3 + m_k y + n_k = 0,$$

where

$$m_k = \frac{e_2^k}{2} - \frac{3}{16} e_3^{k2}, \quad n_k = \frac{e_3^{k3}}{32} - \frac{e_3^k e_2^k}{8} + \frac{e_1^k}{4}.$$

Define

$$W_k = \left(\frac{n_k}{2} \right)^2 + \left(\frac{m_k}{3} \right)^3, \quad \sigma = \frac{-1 + i\sqrt{3}}{2}, \tag{14}$$

$$\begin{aligned}
 y_1 &= \sqrt[3]{-\frac{n_k}{2} + \sqrt{W_k}} + \sqrt[3]{-\frac{n_k}{2} - \sqrt{W_k}}, \\
 y_2 &= \sqrt[3]{-\frac{n_k}{2} + \sqrt{W_k}\sigma} + \sqrt[3]{-\frac{n_k}{2} - \sqrt{W_k}\sigma^2}, \\
 y_3 &= \sqrt[3]{-\frac{n_k}{2} + \sqrt{W_k}\sigma^2} + \sqrt[3]{-\frac{n_k}{2} - \sqrt{W_k}\sigma}, \\
 z_{kj} &= y_j - \frac{e_3^k}{4}, \quad j = 1, 2, 3.
 \end{aligned}
 \tag{15}$$

Lemma 5. $h(z_k) = 0$ has at least one positive root if and only if one of the following conditions is satisfied, where r_k, q_k, h_k are defined in (6), and W_k ($k \in \mathbb{N}_0$) and z_{kj} ($1 \leq j \leq 3$) are defined as in (14) and (15), respectively:

- (H1) $(r_k + h_k - q_k)(r_k + h_k + q_k) < 0$;
- (H2) $(r_k + h_k - q_k)(r_k + h_k + q_k) \geq 0, W_k \geq 0, z_{k1} > 0,$ and $h(z_{k1}) \leq 0$;
- (H3) $(r_k + h_k - q_k)(r_k + h_k + q_k) \geq 0, W_k < 0,$ there exists at least one $z^* \in \{z_{k1}, z_{k2}, z_{k3}\}$ such that $z^* > 0$ and $h(z^*) \leq 0$.

Remark 2. By Routh–Hurwitz stability criterion it is easy to prove that there exists a $K_0 \in \mathbb{N}_0$ such that (12) has no positive roots for $k > K_0$. In other words, (12) exists positive roots only possible for a finite number of $0 \leq k \leq K_0$.

Denote

$$\mathcal{K} := \{k \in \mathbb{N}_0 \mid 0 \leq k \leq K_0 \text{ and one of conditions (H1), (H2) and (H3) holds}\}.$$

Suppose \mathcal{K} is not empty, and without loss of generality, we assume that it has four positive roots denoted by $z_{k,l}, k \in \mathcal{K}, l = 1, 2, 3, 4$. Then (11) has four positive roots, say $w_{k,l} = \sqrt{z_{k,l}}, k \in \mathcal{K}, l = 1, 2, 3, 4$.

Let

$$\tau_{k,l}^{(j)} = \begin{cases} \frac{2 \arctan \theta_{k,l} + 2j\pi}{\omega_{k,l}}, & k \in \mathcal{K}, j \in \mathbb{N}_0, l = 1, 2, 3, 4, \quad \text{if } \theta_{k,l} \geq 0, \\ \frac{2 \arctan \theta_{k,l} + 2(j+1)\pi}{\omega_{k,l}}, & k \in \mathcal{K}, j \in \mathbb{N}_0, l = 1, 2, 3, 4, \quad \text{if } \theta_{k,l} < 0. \end{cases}$$

Then $\pm iw_{k,l}$ is a pair of purely imaginary roots of (5) with $\tau = \tau_{k,l}^{(j)}$, i.e.,

$$\lambda(\tau) = \alpha(\tau) + i\omega(\tau)$$

be the root of (5) near $\tau = \tau_{k,l}^{(j)}$ satisfying

$$\alpha(\tau_{k,l}^{(j)}) = 0, \quad \omega(\tau_{k,l}^{(j)}) = w_{k,l}.$$

Clearly, the sequence $\{\tau_{k,l}^{(j)}\}_{j=0}^{+\infty}$ is increasing in j , and

$$\lim_{j \rightarrow +\infty} \tau_{k,l}^{(j)} = +\infty, \quad l = 1, 2, 3, 4.$$

Thus, we can define

$$\begin{aligned} \tau_* &:= \tau_{k_2, l_0}^{(0)} := \min\{\tau_{k, l}^{(0)} : l = 1, 2, 3, 4; k \in \mathcal{K}\}, \\ w_* &:= w_{k_2, l_0}, \\ \theta_* &\text{ is the real root of (8) with } w_k = w_*. \end{aligned} \tag{16}$$

From the above analysis we arrive at the following conclusion on the Hopf bifurcation of system (3).

Theorem 2. *Assume that (N0) and $\varepsilon > \varepsilon_*(D)$ are satisfied. τ_* , θ_* , ω_* , k_2 and l_0 are defined as in (16).*

- (i) *If none of (H1)–(H3) in Lemma 5 is satisfied, then all the roots of (5) have negative real parts for all $\tau \geq 0$. Therefore, equilibrium point (u_*, v_*) of system (2) is asymptotically stable;*
- (ii) *If one of (H1)–(H3) in Lemma 5 is satisfied, then (12) has at least one positive root, all the roots of (5) have negative real parts when $\tau \in [0, \tau_*)$. Moreover, if $\tau_* < \infty$, $\mathcal{G}(\theta_*, \omega_*) \neq 0$, and $\tau_{k, j}^0 \neq \tau_*$ for $k \neq k_2$ and $i \neq j_0$, then when $\tau = \tau_*$, all the roots of (5) have negative real parts except a pair of simple purely imaginary roots $\pm i\omega_*$, system (2) undergoes k_2 -mode Hopf bifurcation near (u_*, v_*) , and for $\tau \in (\tau_*, \tau_* + \epsilon)$ with some small $\epsilon > 0$, (5) has exactly one pair of conjugate complex roots with positive real parts.*

3 Turing–Hopf bifurcation

Based on the analysis above, we have obtained the following Turing–Hopf bifurcation theorem.

Theorem 3. *For system (3), assume (N0) holds, $D > \gamma$ and one of conditions (H1)–(H3) in Lemma 5 holds. Given $k_1 \in \mathbb{N}_0$, $k_2 \in \mathcal{K}$. Then the constant steady state (u_*, v_*) is locally asymptotically stable when $\varepsilon > \varepsilon_*(D)$ and $0 \leq \tau < \tau_*$. Moreover, for $D \in (D_{k_1, k_1+1}, D_{k_1-1, k_1})$, system (3) undergoes (k_1, k_2) -mode Turing–Hopf bifurcation near (u_*, v_*) at $(\tau, \varepsilon) = (\tau_*, \varepsilon_*(D)) := (\tau_*, \varepsilon_*(D))$.*

In the following, we consider the spatiotemporal pattern of system (3) induced by Turing–Hopf bifurcation. We apply the method in [11] to calculate the normal forms of Turing–Hopf bifurcation for (τ, ε) near the bifurcation point (τ_*, ε_*) . First, normalize the delay τ in system (3) by time scaling $t \rightarrow t/\tau$ and translate (u_*, v_*) into origin. Then system (3) can be translated into

$$\begin{aligned} \frac{\partial u(x, t)}{\partial t} &= \tau \left[\varepsilon D \frac{\partial^2 u(x, t)}{\partial x^2} + \gamma \left(p - q(u(x, t) + u_*) + \frac{(u(x, t-1) + u_*)^2}{v(x, t-1) + v_*} \right) \right], \\ \frac{\partial v(x, t)}{\partial t} &= \tau \left[D \frac{\partial^2 v(x, t)}{\partial x^2} + \gamma \left((u(x, t-1) + u_*)^2 - (v(x, t) + v_*) \right) \right]. \end{aligned} \tag{17}$$

First of all, we define the following real-value Hilbert space

$$X := \{(u, v) \in H^2(0, l\pi) \times H^2(0, l\pi): (u_x, v_x)|_{x=0, l\pi} = 0\},$$

where $H^2(0, l\pi)$ is a standard Sobolev space, and the corresponding complexification is $X_{\mathbb{C}} := \{x_1 + ix_2: x_1, x_2 \in X\}$, with the complex valued L^2 inner product

$$\langle U_1, U_2 \rangle = \int_0^{l\pi} (\bar{u}_1 u_2 + \bar{v}_1 v_2) dx, \quad U_i = (u_i, v_i) \in X_{\mathbb{C}}.$$

Let $\mathcal{C} := C([-1, 0], X_{\mathbb{C}})$ denote the phase space with the sup norm. We write $\varphi_t \in \mathcal{C}$ for $\varphi_t(\theta) = \varphi(t + \theta)$, $-1 \leq \theta \leq 0$.

According to [11], system (17) can be rewritten as

$$\frac{d}{dt}U(t) = D(\alpha)\Delta U(t) + L(\alpha)(U_t) + F(\alpha, U_t), \tag{18}$$

where $\alpha = (\alpha_1, \alpha_2) = (\tau - \tau_*, \varepsilon - \varepsilon_*)$, $D(\alpha) = \text{diag}(\tau\varepsilon D, \tau D)$, $U = (u, v)^T \in X_{\mathbb{C}}$, $U_t = (u_t, v_t)^T \in \mathcal{C}$. $L: \mathbb{R}^2 \times \mathcal{C} \rightarrow X_{\mathbb{C}}$ is a bounded linear operator. $F: \mathbb{R}^2 \times \mathcal{C} \rightarrow X_{\mathbb{C}}$ is a C^k ($k \geq 3$) function and satisfies $F(0, 0) = 0$, $D_{\varphi}F(0, 0) = 0$ with $\varphi \in \mathcal{C}$.

From (18) we can obtain that

$$\begin{aligned} D(0) &= \tau_* D \begin{pmatrix} \varepsilon_* & 0 \\ 0 & 1 \end{pmatrix}, \\ D_1(\alpha) &= 2D \begin{pmatrix} \tau_*\alpha_2 + \alpha_1\varepsilon_* & 0 \\ 0 & \alpha_1 \end{pmatrix}, \\ L_0\varphi &= \tau_*\gamma \begin{pmatrix} -q\varphi_1(0) + \frac{2}{u_*}\varphi_1(-1) - \frac{1}{u_*^2}\varphi_2(-1) \\ -\varphi_2(0) + 2u_*\varphi_1(-1) \end{pmatrix}, \\ L_1(\alpha)\varphi &= 2\alpha_1\gamma \begin{pmatrix} -q\varphi_1(0) + \frac{2}{u_*}\varphi_1(-1) - \frac{1}{u_*^2}\varphi_2(-1) \\ -\varphi_2(0) + 2u_*\varphi_1(-1) \end{pmatrix}, \\ Q(\varphi, \varphi) &= 2\tau_*\gamma \begin{pmatrix} \frac{1}{v_*}\varphi_1^2(-1) - \frac{2}{u_*^3}\varphi_1(-1)\varphi_2(-1) + \frac{1}{u_*^4}\varphi_2^2(-1) \\ \varphi_1^2(-1) \end{pmatrix}, \\ C(\varphi, \varphi, \varphi) &= 6\tau_*\gamma \begin{pmatrix} -\frac{1}{v_*^2}\varphi_1^2(-1)\varphi_2(-1) + \frac{2}{u_*^5}\varphi_1(-1)\varphi_2^2(-1) - \frac{1}{u_*^6}\varphi_2^3(-1) \\ 0 \end{pmatrix} \end{aligned} \tag{19}$$

with $\varphi = (\varphi_1, \varphi_2)^T$, $\alpha = (\alpha_1, \alpha_2)^T$, $Q(\varphi, \varphi)$ and $C(\varphi, \varphi, \varphi)$ are the second and third Fréchet derivative of $F(\alpha, \varphi)$ at $\alpha = 0$, respectively.

By (2.4), (2.6), (2.7), (2.9) and (2.10) of [11] we can get that

$$\begin{aligned} \phi_1(\theta) &= (1, p_1)^T, & \phi_2(\theta) &= e^{i\omega_*\tau_*\theta}(1, p_2)^T, \\ \psi_1(s) &= N_1(1, q_1), & \psi_2(s) &= e^{-i\omega_*\tau_*s}N_2(1, q_2) \end{aligned} \tag{20}$$

with

$$\begin{aligned}
 p_1 &= -\frac{(p+1)^2}{\gamma q^2} \left(\varepsilon_* D k_1^2 + \gamma q - \frac{2\gamma q}{p+1} \right), \\
 p_2 &= \frac{(p+1)^2}{\gamma q^2} \left(-i w_* - \varepsilon_* D k_2^2 - \gamma q + \frac{2\gamma q}{p+1} e^{-i w_* \tau_*} \right) e^{i w_* \tau_*}, \\
 q_1 &= \frac{q}{2\gamma(p+1)} \left(\varepsilon_* D k_1^2 + \gamma q - \frac{2\gamma q}{p+1} \right), \\
 q_2 &= \frac{q}{2\gamma(p+1)} \left(i w_* + \varepsilon_* D k_2^2 + \gamma q - \frac{2\gamma q}{p+1} e^{-i w_* \tau_*} \right) e^{i w_* \tau_*}, \\
 N_1 &= \left[\left(-\frac{\tau_* \gamma q^2}{(p+1)^2} + q_1 \right) p_1 + \frac{2\gamma \tau_* q}{p+1} + \frac{2\tau_* \gamma (p+1)}{q} q_1 + 1 \right]^{-1}, \\
 N_2 &= \left[p_2 q_1 + 1 + e^{-i w_* \tau_*} \left(\frac{2\gamma \tau_* q}{p+1} + \frac{2\tau_* \gamma (p+1)}{q} q_2 - p_2 \frac{\tau_* \gamma q^2}{(p+1)^2} \right) \right]^{-1}.
 \end{aligned}$$

For $\alpha = (\alpha_1, \alpha_2)$ in a small neighbourhood of $(0, 0)$, it follows from [11] that the normal forms of (18) for $\Omega = (0, \pi)$ up to the third order are

$$\begin{aligned}
 \dot{z}_1 &= a_1(\alpha) z_1 + a_{11} z_1^2 + a_{23} z_2 \bar{z}_2 + a_{111} z_1^3 + a_{123} z_1 z_2 \bar{z}_2 + \text{h.o.t}, \\
 \dot{z}_2 &= i w_0 z_2 + b_2(\alpha) z_2 + b_{12} z_1 z_2 + b_{112} z_1^2 z_2 + b_{223} z_2^2 \bar{z}_2 + \text{h.o.t}, \\
 \dot{\bar{z}}_2 &= -i w_0 \bar{z}_2 + \overline{b_2(\alpha)} \bar{z}_2 + \overline{b_{12}} z_1 \bar{z}_2 + \overline{b_{112}} z_1^2 \bar{z}_2 + \overline{b_{223}} z_2 \bar{z}_2^2 + \text{h.o.t}.
 \end{aligned} \tag{21}$$

According to [11], the coefficients in (21) can be calculated by the following lemma in the case of $k_2 = 0, k_1 \neq 0$ (which is referred to Turing–Hopf bifurcation of Hopf–Pitchfork type).

Lemma 6. (See [11].) For $k_2 = 0, k_1 \neq 0$, the parameters $a_1(\alpha), b_2(\alpha), a_{11}, a_{23}, a_{111}, a_{123}, b_{12}, b_{112}$ and b_{223} in (21) are given by

$$\begin{aligned}
 a_1(\alpha) &= \frac{1}{2} \psi_1(0) (L_1(\alpha) \phi_1 - \mu_{k_1} D_1(\alpha) \phi_1(0)), \\
 b_2(\alpha) &= \frac{1}{2} \psi_2(0) (L_1(\alpha) \phi_2 - \mu_{k_2} D_1(\alpha) \phi_2(0)), \\
 a_{11} &= a_{23} = b_{12} = 0, \\
 a_{111} &= \frac{1}{4} \psi_1(0) C_{\phi_1 \phi_1 \phi_1} + \frac{1}{\omega_0} \psi_1(0) \operatorname{Re}(i Q_{\phi_1 \phi_2} \psi_2(0)) Q_{\phi_1 \phi_1} \\
 &\quad + \psi_1(0) Q_{\phi_1} \left(h_{200}^0 + \frac{1}{\sqrt{2}} h_{200}^{2k_1} \right), \\
 a_{123} &= \psi_1(0) C_{\phi_1 \phi_2 \bar{\phi}_2} + \frac{2}{\omega_0} \psi_1(0) \operatorname{Re}(i Q_{\phi_1 \phi_2} \psi_2(0)) Q_{\phi_2 \bar{\phi}_2} \\
 &\quad + \psi_1(0) \left[Q_{\phi_1} \left(h_{011}^0 + \frac{1}{\sqrt{2}} h_{011}^{2k_1} \right) + Q_{\phi_2} h_{101}^{k_1} + Q_{\bar{\phi}_2} h_{110}^{k_1} \right],
 \end{aligned}$$

$$\begin{aligned}
 b_{112} &= \frac{1}{2}\psi_2(0)C_{\phi_1\phi_1\phi_2} + \frac{1}{2i\omega_0}\psi_2(0)\{2Q_{\phi_1\phi_1}\psi_1(0)Q_{\phi_1\phi_2} \\
 &\quad + [-Q_{\phi_2\phi_2}\psi_2(0) + Q_{\phi_2\bar{\phi}_2}\bar{\psi}_2(0)]Q_{\phi_1\phi_1}\} + \psi_2(0)(Q_{\phi_1}h_{110}^{k_1} + Q_{\phi_2}h_{200}^0), \\
 b_{223} &= \frac{1}{2}\psi_2(0)C_{\phi_2\phi_2\bar{\phi}_2} + \frac{1}{4i\omega_0}\psi_2(0)\left\{\frac{2}{3}Q_{\bar{\phi}_2\bar{\phi}_2}\bar{\psi}_2(0)Q_{\phi_2\phi_2} + [-2Q_{\phi_2\phi_2}\psi_2(0) \right. \\
 &\quad \left. + 4Q_{\phi_2\bar{\phi}_2}\bar{\psi}_2(0)]Q_{\phi_2\bar{\phi}_2}\right\} + \psi_2(0)(Q_{\phi_2}h_{011}^0 + Q_{\bar{\phi}_2}h_{020}^0),
 \end{aligned}$$

where

$$h_{200}^0(\theta) = -\frac{1}{2}\left[\int_{-r}^0 d\eta_0(\theta)\right]^{-1} Q_{\phi_1\phi_1} + \frac{1}{2i\omega_0}(\phi_2(\theta)\psi_2(0) - \bar{\phi}_2(\theta)\bar{\psi}_2(0))Q_{\phi_1\phi_1},$$

$$h_{200}^{2k_1}(\theta) = -\frac{1}{2\sqrt{2}}\left[\int_{-r}^0 d\eta_{2k_1}(\theta)\right]^{-1} Q_{\phi_1\phi_1},$$

$$h_{011}^0(\theta) = -\left[\int_{-r}^0 d\eta_0(\theta)\right]^{-1} Q_{\phi_2\bar{\phi}_2} + \frac{1}{i\omega_0}(\phi_2(\theta)\psi_2(0) - \bar{\phi}_2(\theta)\bar{\psi}_2(0))Q_{\phi_2\bar{\phi}_2},$$

$$h_{011}^{2k_1}(\theta) = 0,$$

$$\begin{aligned}
 h_{020}^0(\theta) &= \frac{1}{2}\left[2i\omega_0 I - \int_{-r}^0 e^{2i\omega_0\theta} d\eta_0(\theta)\right]^{-1} Q_{\phi_2\phi_2} e^{2i\omega_0\theta} \\
 &\quad - \frac{1}{2i\omega_0}\left[\phi_2(\theta)\psi_2(0) + \frac{1}{3}\bar{\phi}_2(\theta)\bar{\psi}_2(0)\right]Q_{\phi_2\phi_2},
 \end{aligned}$$

$$h_{110}^{k_1}(\theta) = \left[i\omega_0 I - \int_{-r}^0 e^{i\omega_0\theta} d\eta_{k_1}(\theta)\right]^{-1} Q_{\phi_1\phi_2} e^{i\omega_0\theta} - \frac{1}{i\omega_0}\phi_1(0)\psi_1(0)Q_{\phi_1\phi_2},$$

$$h_{002}^0(\theta) = \overline{h_{020}^0(\theta)}, \quad h_{101}^{k_1}(\theta) = \overline{h_{110}^{k_1}(\theta)},$$

$\theta \in [-r, 0]$, $\eta_k \in BV([-r, 0], \mathbb{C}^m)$ is denoted by [11, (2.6)], that is,

$$-\mu_k D_0\psi(0) + L_0\psi = \int_{-r}^0 d\eta_k(\theta)\psi(\theta), \quad \psi \in C \triangleq C([-r, 0], \mathbb{C}^m), \quad k \in \mathbb{N}_0,$$

and the other notations are given by (19) and (20).

4 Spatiotemporal patterns with Turing–Hopf bifurcation

In the following, we will give examples to illustrate the various spatiotemporal patterns of system (3) with a fixed set of parameter values.

4.1 (1,0)-mode Turing–Hopf bifurcation

Referring to [15], choose $k_1 = 1$, $p = 0.1$, $q = 0.8$, $\gamma = 0.1$, diffusion coefficient $D = 0.5$. We can obtain $(u_*, v_*) = (1.375, 1.8906)$ and $\varepsilon_*(0.5) = 0.0824$. Then 1-mode Turing bifurcation of (3) will occur at $\varepsilon_*(0.5) = 0.0824$. Through numerical simulation, we can know that $w_* = 0.0721$ and $\tau_* = 2.6753$.

Furthermore, under the above given parameters, normal form for (1, 0)-mode Turing–Hopf bifurcation truncated to order 3 is

$$\begin{aligned} \dot{z}_1 &= (0.0000994925\alpha_1 - 1.0974\alpha_2)z_1 - 0.052899z_1^3 - 0.046137z_1z_2\bar{z}_2 \\ \dot{z}_2 &= 0.0721iz_2 + (0.009913 + 0.056380i)\alpha_1z_2 + (-0.003850 + 0.037100i)z_1^2z_2 \\ &\quad + (-0.001136 - 0.034234i)z_2^2\bar{z}_2 \\ \dot{\bar{z}}_2 &= -0.0721i\bar{z}_2 + (0.009913 - 0.056380i)\alpha_1\bar{z}_2 + (-0.003850 - 0.037100i)z_1^2\bar{z}_2 \\ &\quad + (-0.001136 + 0.034234i)z_2\bar{z}_2^2. \end{aligned}$$

In addition, the equivalent planar system is

$$\begin{aligned} \dot{r} &= r(-0.00991322\alpha_1 + r^2 + 0.072772z^2), \\ \dot{z} &= z(-0.000094925\alpha_1 + 1.09741\alpha_2 + 40.626331r^2 + z^2). \end{aligned} \tag{22}$$

According to [7], the unfolding for (22) is case Ib. The bifurcation set for system (3) in ε, τ -plane is shown in Fig. 2(a), where the critical bifurcation lines are

$$\begin{aligned} \mathcal{L}_1: \quad &\varepsilon = \varepsilon_* + 0.000009066(\tau - \tau_*), & \tau < \tau_*, \\ \mathcal{L}_2: \quad &\tau = \tau_*, & \varepsilon < \varepsilon_*, \\ \mathcal{L}_3: \quad &\varepsilon = \varepsilon_* - 0.366980(\tau - \tau_*), & \tau > \tau_*, \\ \mathcal{L}_4: \quad &\varepsilon = \varepsilon_* - 0.124122(\tau - \tau_*), & \tau > \tau_*, \\ \mathcal{L}_5: \quad &\varepsilon = \varepsilon_* + 0.000009066(\tau - \tau_*), & \tau > \tau_*, \\ \mathcal{L}_6: \quad &\tau = \tau_*, & \varepsilon > \varepsilon_*. \end{aligned}$$

Therefore, the τ, ε -plane is divided into six regions by critical bifurcation curves \mathcal{L}_i , $i = 1, 2, \dots, 6$, which are denoted by \mathcal{D}_i , $i = 1, 2, \dots, 6$. For (τ, ε) in different region \mathcal{D}_i , $i = 1, 2, \dots, 6$, the dynamical behaviors of (22) can be described by corresponding phase portraits; see Fig. 2(b).

Theorem 4. For system (3) with $p = 0.1$, $q = 0.8$, $\gamma = 0.1$ and $D = 0.5$, when parameters (τ, ε) are chosen near Turing–Hopf bifurcation point $(\tau_*, \varepsilon_*) = (0.0824, 2.6753)$, system (3) exhibits the following complex dynamics:

- (i) When $(\tau, \varepsilon) \in \mathcal{D}_1$, the steady state (u_*, v_*) of system (3) is asymptotically stable. Otherwise, the steady state (u_*, v_*) is unstable, while $(\tau, \varepsilon) \notin \bar{\mathcal{D}}_1$.
- (ii) When $(\tau, \varepsilon) \in \mathcal{D}_2$, system (3) possesses a pair of stable spatially inhomogeneous steady states through Turing bifurcation at (u_*, v_*) when (τ, ε) crosses \mathcal{L}_1 , which reflects that system exhibits spatial patterns and bistability.

- (iii) When $(\tau, \varepsilon) \in \mathcal{D}_3$, there are a pair of stable spatially inhomogeneous steady states and an unstable spatially homogeneous periodic solution for system (3). Moreover, there exist a pair of heteroclinic orbits, which connect the spatially homogeneous periodic solution to spatially inhomogeneous steady states, respectively. That is, the system exhibits semistable patterns and bistability.
- (iv) When $(\tau, \varepsilon) \in \mathcal{D}_4$, there are two unstable spatially inhomogeneous periodic solution, which are bifurcated from the spatially homogeneous periodic orbit on \mathcal{L}_3 , and a pair of spatially inhomogeneous steady states, and a spatially homogeneous periodic solution for system (3) still remains. Moreover, there are four heteroclinic orbits connecting spatially inhomogeneous periodic solution to the spatially homogeneous periodic solution and spatially inhomogeneous steady states, respectively. Therefore, system shows semistable spatiotemporal patterns and tristability; see Fig. 3.
- (v) When $(\tau, \varepsilon) \in \mathcal{D}_5$, system (3) possesses a stable spatially homogeneous periodic solution and a pair of unstable spatially inhomogeneous steady states. Moreover, there are a pair of heteroclinic orbits connecting spatially inhomogeneous steady states to the spatially homogeneous periodic solution, respectively, which reflects that system exhibits semistable patterns and bistability.
- (vi) When $(\tau, \varepsilon) \in \mathcal{D}_6$, system (3) has a stable spatially homogeneous periodic solution, which represents that system exhibits temporal patterns.

4.2 (2,0)-mode Turing–Hopf bifurcation

In this part, we select $k_1 = 2, p = 0.1, q = 0.8, \gamma = 0.1, D = 0.15$. Then $(u_*, v_*) = (1.375, 1.8906), \varepsilon_*(0.15) = 0.0745, w_* = 0.0721$ and $\tau_* = 2.6753$. According to [7], the unfolding for the cylindrical coordinate equation of (21) is case III. When $(\tau, \varepsilon) = (2.7253, 0.0445)$, there are two spatially inhomogeneous periodic solutions; see Fig. 4. If $(\tau, \varepsilon) = (2.6253, 0.0705)$, two spatially inhomogeneous steady states coexist; see Fig. 5. It is easy to observe that the patterns are different from the last case.

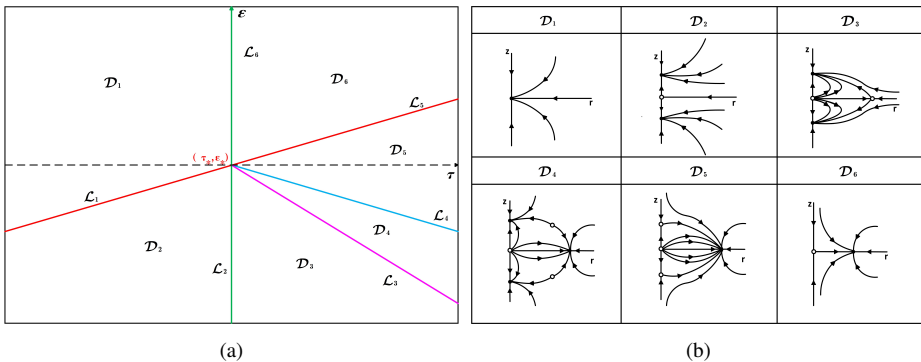


Figure 2. (a) The bifurcation set of (22) in τ, ε -plane. (b) The phase portraits of (22) in case Ib.

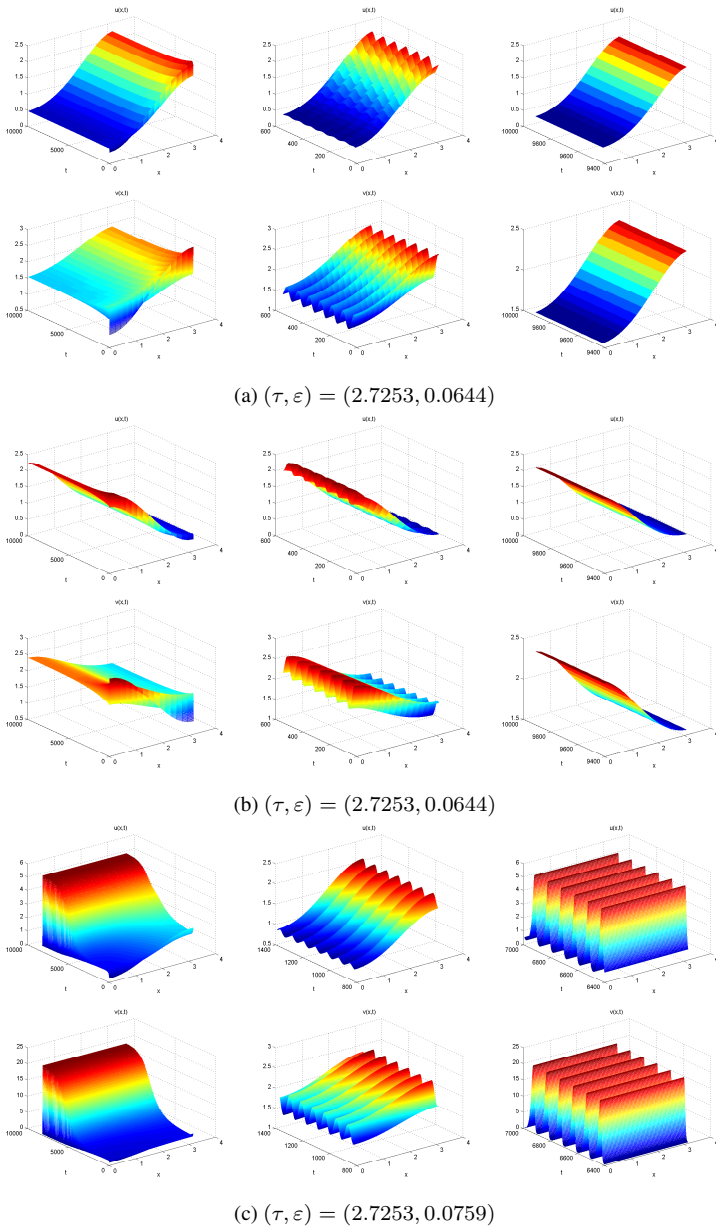


Figure 3. For $(\tau, \varepsilon) \in \mathcal{D}_4$, a pair of spatially inhomogeneous steady states and a spatially homogeneous periodic solution are stable. There are semistable patterns of spatially inhomogeneous periodic solutions tending toward spatially inhomogeneous steady states and spatially homogeneous periodic solution, respectively. The initial functions are: (a) $\phi_1(x, t) = 1.35 - \cos x$, $\phi_2(x, t) = 1.9 - \cos x$, $(x, t) \in [0, \pi] \times [-2.7253, 0]$; (b) $\phi_1(x, t) = 1.35 + \cos x$, $\phi_2(x, t) = 1.9 + \cos x$, $(x, t) \in [0, \pi] \times [-2.7253, 0]$; (c) $\phi_1(x, t) = 1.3 - \cos x$, $\phi_2(x, t) = 1.9 - \cos x$, $(x, t) \in [0, \pi] \times [-2.7253, 0]$.

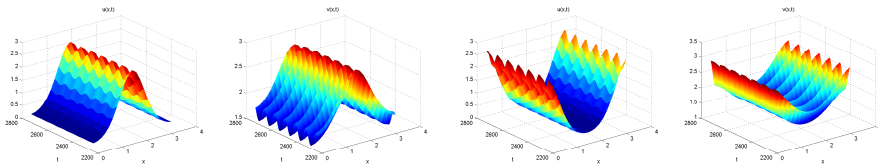


Figure 4. For $(\tau, \varepsilon) = (2.7253, 0.0445)$, a pair of spatially inhomogeneous periodic solution are stable. The initial functions are $\phi_1(x, t) = 1.375 - \cos 2x$, $\phi_2(x, t) = 1.8906 - 1.7 \cos 2x$ for $(x, t) \in [0, \pi] \times [-2.7253, 0]$.

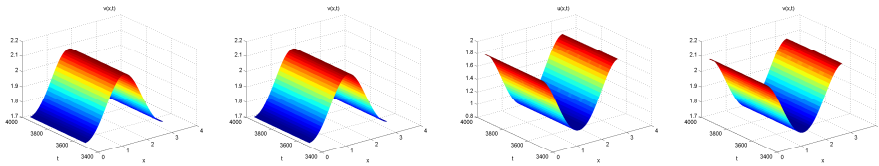


Figure 5. For $(\tau, \varepsilon) = (2.6253, 0.0705)$, a pair of spatially inhomogeneous steady states are stable. The initial functions are $\phi_1(x, t) = 1.375 - \cos 2x$, $\phi_2(x, t) = 1.8906 - 1.7 \cos 2x$ for $(x, t) \in [0, \pi] \times [-2.6253, 0]$.

5 Conclusion

In this paper, we have built the existence conditions of Turing, Hopf and Turing–Hopf bifurcation for Gierer–Meinhardt system with gene expression delay. The first Turing bifurcation curve $\varepsilon_*(D)$ is given, which is continuous and piecewise smooth, and at nonsmooth points system (3), has undergone Turing–Turing bifurcation. Besides, it has found that diffusion can induce Turing instability, resulting in spatially nonhomogeneous steady states.

Using τ as bifurcation parameter, we have further investigated the Hopf bifurcation for system (3) near (u_*, v_*) . Based on the method of [2] and [17], we have overcome the complexity of solving the purely imaginary roots for a second-order transcendental polynomial and given the critical values τ for the occurrence of Hopf bifurcation at which spatially homogeneous periodic solution will be bifurcated from (u_*, v_*) .

In order to explore the joint effect of diffusion and time delay, we further investigate the Turing–Hopf bifurcation. Utilizing the general formula established in [11], we have derived the normal form for system (3) near the Turing–Hopf singularity. It is theoretically proved that system exhibits spatial, temporal and spatiotemporal patterns, such as semistable spatially inhomogeneous periodic solutions, as well as tristable phenomena of a pair of stable spatially inhomogeneous steady states and a spatially homogeneous periodic solution coexisting, which is not found in the another representative Turing model, Schnakenberg system [12]. Significantly, the morphogenetic system can delineate the patterns of animal epidermis, as a consequence, various spatiotemporal patterns provide an explanation for the appearance of animal epidermal patterns. Our research provide an analytical means for understanding the behavior of delayed biological self-organizing systems and the parameter space for when bifurcations occur. The analysis have shown

that Turing–Hopf bifurcation provides an explanation for the formation of spatiotemporal pattern. The numerical results well confirmed the frontal theoretical analyses.

Lee et al. have found that the inclusion of time delay induces the generation of oscillation patterns [15, Fig. 5 A, C or Fig. 5 D, F or Fig. 6 D, E], which can be explained by Hopf bifurcation taking time delay as the parameter. Furthermore, time delay will greatly postpone the formation of the pattern [15, Fig. 5 A, B], which is also confirmed in our research. By analyzing the phase portraits near the Turing–Hopf singularity of the system ($\mathcal{D}_3 - \mathcal{D}_4$) we find that the introduction of time delay result in there are semistable patterns from spatially homogeneous periodic solution (or spatially nonhomogeneous periodic solution bifurcated from spatially homogeneous periodic solution) to spatially nonhomogeneous steady state, which attract its nearby solutions, therefore, the occurrence of the semistable patterns will postpone the time to reach the heterogeneous steady pattern. In addition, it is known from Theorem 1 that Turing–Turing bifurcation will occur in model (3). Such kind of degenerate bifurcation is usually used to explain the formation of the superposition of spatial patterns.

References

1. X. Cao, W. Jiang, Turing–Hopf bifurcation and spatiotemporal patterns in a diffusive predator–prey system with Crowley–Martin functional response, *Nonlinear Anal., Real World Appl.*, **43**:428–450, 2018, <https://doi.org/10.1016/j.nonrwa.2018.03.010>.
2. S. Chen, J. Shi, J. Wei, Time delay-induced instabilities and Hopf bifurcations in general reaction–diffusion systems, *J. Nonlinear Sci.*, **23**(1):1–38, 2012, <https://doi.org/10.1007/s00332-012-9138-1>.
3. Y. Ding, W. Jiang, P. Yu, Bifurcation analysis in a recurrent neural network model with delays, *Commun. Nonlinear Sci. Numer. Simul.*, **18**(2):351–372, 2013, <https://doi.org/10.1016/j.cnsns.2012.07.002>.
4. T. Faria, Normal forms and Hopf bifurcation for partial differential equations with delays, *Trans. Am. Math. Soc.*, **352**(5):2217–2239, 2000, <https://doi.org/10.1090/S0002-9947-00-02280-7>.
5. T. Faria, W. Huang, J. Wu, Smoothness of center manifolds for maps and formal adjoints for semilinear FDEs in general Banach spaces, *SIAM J. Math. Anal.*, **34**(1):173–203, 2002, <https://doi.org/10.1137/S0036141001384971>.
6. A. Gierer, H. Meinhardt, A theory of biological pattern formation, *Kybernetik*, **12**(1):30–39, 1972, <https://doi.org/10.1007/BF00289234>.
7. J. Guckenheimer, P. Holmes, *Nonlinear Oscillations, Dynamical Systems, and Bifurcations of Vector Fields*, Springer, New York, 1983, <https://doi.org/10.1007/978-1-4612-1140-2>.
8. S. Guo, Stability and bifurcation in a reaction–diffusion model with nonlocal delay effect, *J. Differ. Equations*, **259**(4):1409–1448, 2015, <https://doi.org/10.1016/j.jde.2015.03.006>.
9. J. Gurdon, P. Bourillot, Morphogen gradient interpretation, *Nature*, **413**(6858):797–803, 2001, <https://doi.org/10.1038/35101500>.

10. J. Hale, *Theory of Functional Differential Equations*, Springer, New York, 1977, <https://doi.org/10.1007/978-1-4612-9892-2>.
11. W. Jiang, Q. An, J. Shi, Formulation of the normal form of Turing–Hopf bifurcation in partial functional differential equations, *J. Differ. Equations*, **268**(10):6067–6102, 2019, <https://doi.org/10.1016/j.jde.2019.11.039>.
12. W. Jiang, H. Wang, X. Cao, Turing instability and Turing–Hopf bifurcation in diffusive Schnakenberg systems with gene expression time delay, *J. Dyn. Differ. Equations*, **31**(4):2223–2247, 2018, <https://doi.org/10.1007/s10884-018-9702-y>.
13. A. Koch, H. Meinhardt, Biological pattern formation: From basic mechanisms to complex structures, *Rev. Mod. Phys.*, **66**(4):1481–1507, 1994, <https://doi.org/10.1103/RevModPhys.66.1481>.
14. S. Lee, E. Gaffney, R. Baker, The dynamics of Turing patterns for morphogen-regulated growing domains with cellular response delays, *Bull. Math. Biol.*, **73**(11):2527–2551, 2011, <https://doi.org/10.1007/s11538-011-9634-8>.
15. S. Lee, E. Gaffney, N. Monk, The influence of gene expression time delays on Gierer–Meinhardt pattern formation systems, *Bull. Math. Biol.*, **72**(8):2139–2160, 2010, <https://doi.org/10.1007/s11538-010-9532-5>.
16. J. Lewis, Autoinhibition with transcriptional delay: A simple mechanism for the zebrafish somitogenesis oscillator, *Curr. Biol.*, **13**(16):1398–1408, 2003, [https://doi.org/10.1016/S0960-9822\(03\)00534-7](https://doi.org/10.1016/S0960-9822(03)00534-7).
17. X. Li, J. Wei, On the zeros of a fourth degree exponential polynomial with applications to a neural network model with delays, *Chaos Solitons Fractals*, **26**(2):519–526, 2005, <https://doi.org/10.1016/j.chaos.2005.01.019>.
18. J. Liu, F. Yi, J. Wei, Multiple bifurcation analysis and spatiotemporal patterns in a 1-D Gierer–Meinhardt model of morphogenesis, *Int. J. Bifurcation Chaos Appl. Sci. Eng.*, **20**(4):1007–1025, 2010, <https://doi.org/10.1142/S0218127410026289>.
19. J. Liu, X. Zhang, Stability and Hopf bifurcation of a delayed reaction–diffusion predator–prey model with anti-predator behaviour, *Nonlinear Anal. Model. Control*, **24**(3):387–406, 2019, <https://doi.org/10.15388/NA.2019.3.5>.
20. I. Ncube, On the stability and Hopf bifurcation of the non-zero uniform endemic equilibrium of a time-delayed malaria model, *Nonlinear Anal. Model. Control*, **21**(6):851–860, 2016, <https://doi.org/10.15388/NA.2016.6.8>.
21. S. Ruan, Diffusion-driven instability in the Gierer–Meinhardt model of morphogenesis, *Nat. Resour. Model.*, **11**(2):131–141, 1998, <https://doi.org/10.1111/j.1939-7445.1998.tb00304.x>.
22. R. Sakuma, Y. Ohnishi, C. Meno, H. Fujii, H. Juan, J. Takeuchi, T. Ogura, E. Li, K. Miyazono, H. Hamada, Inhibition of Nodal signalling by Lefty mediated through interaction with common receptors and efficient diffusion, *Genes Cells*, **7**(4):401–412, 2002, <https://doi.org/10.1046/j.1365-2443.2002.00528.x>.
23. J. Schnakenberg, Simple chemical reaction systems with limit cycle behaviour, *J. Theor. Biol.*, **81**(3):389–400, 1979, [https://doi.org/10.1016/0022-5193\(79\)90042-0](https://doi.org/10.1016/0022-5193(79)90042-0).
24. Y. Song, H. Jiang, Q. Liu, Y. Yuan, Spatiotemporal dynamics of the diffusive mussel–algae model near Turing–Hopf bifurcation, *SIAM J. Appl. Dyn. Syst.*, **16**(4):2030–2062, 2017, <https://doi.org/10.1137/16M1097560>.

25. Y. Su, X. Zou, Transient oscillatory patterns in the diffusive non-local blowfly equation with delay under the zero-flux boundary condition, *Nonlinearity*, **27**(1):87–104, 2013, <https://doi.org/10.1088/0951-7715/27/1/87>.
26. A. Turing, The chemical basis of morphogenesis, *Philos. Trans. R. Soc. Lond., Ser. B, Biol. Sci.*, **237**(641):37–72, 1952.
27. J. Wu, *Theory and Applications of Partial Functional Differential Equations*, Springer, New York, 1996, <https://doi.org/10.1007/978-1-4612-4050-1>.
28. R. Wu, Y. Zhou, Y. Shao, L. Chen, Bifurcation and Turing patterns of reaction–diffusion activator–inhibitor model, *Physica A*, **462**:597–610, 2017, <https://doi.org/10.1016/j.physa.2017.04.053>.
29. R. Yang, Y. Song, Spatial resonance and Turing–Hopf bifurcations in the Gierer–Meinhardt model, *Nonlinear Anal., Real World Appl.*, **31**:356–387, 2016, <https://doi.org/10.1016/j.nonrwa.2016.02.006>.
30. F. Yi, J. Wei, J. Shi, Bifurcation and spatiotemporal patterns in a homogeneous diffusive predator–prey system, *J. Differ. Equations*, **246**(5):1944–1977, 2009, <https://doi.org/10.1016/j.jde.2008.10.024>.